

ARMY RESEARCH LABORATORY



**Stability of Robotic Path Tracking
Part I. One-Dimensional Scalar Models**

by Michael Grinfeld and Scott Schoenfeld

ARL-TR-3646

September 2005

NOTICES

Disclaimers

The findings in this report are not to be construed as an official Department of the Army position unless so designated by other authorized documents.

Citation of manufacturer's or trade names does not constitute an official endorsement or approval of the use thereof.

Destroy this report when it is no longer needed. Do not return it to the originator.

Army Research Laboratory

Aberdeen Proving Ground, MD 21005-5066

ARL-TR-3646

September 2005

Stability of Robotic Path Tracking Part I. One-Dimensional Scalar Models

**Michael Grinfeld and Scott Schoenfeld
Weapons and Materials Research Directorate, ARL**

REPORT DOCUMENTATION PAGE				<i>Form Approved OMB No. 0704-0188</i>
Public reporting burden for this collection of information is estimated to average 1 hour per response, including the time for reviewing instructions, searching existing data sources, gathering and maintaining the data needed, and completing and reviewing the collection information. Send comments regarding this burden estimate or any other aspect of this collection of information, including suggestions for reducing the burden, to Department of Defense, Washington Headquarters Services, Directorate for Information Operations and Reports (0704-0188), 1215 Jefferson Davis Highway, Suite 1204, Arlington, VA 22202-4302. Respondents should be aware that notwithstanding any other provision of law, no person shall be subject to any penalty for failing to comply with a collection of information if it does not display a currently valid OMB control number. PLEASE DO NOT RETURN YOUR FORM TO THE ABOVE ADDRESS.				
1. REPORT DATE (DD-MM-YYYY) September 2005	2. REPORT TYPE Final		3. DATES COVERED (From - To) 1 October 2004–30 September 2005	
4. TITLE AND SUBTITLE Stability of Robotic Path Tracking Part I. One-Dimensional Scalar Models		5a. CONTRACT NUMBER 5b. GRANT NUMBER 5c. PROGRAM ELEMENT NUMBER		
6. AUTHOR(S) Michael Grinfeld and Scott Schoenfeld		5d. PROJECT NUMBER 622618AH03 5e. TASK NUMBER 5f. WORK UNIT NUMBER		
7. PERFORMING ORGANIZATION NAME(S) AND ADDRESS(ES) U.S. Army Research Laboratory ATTN: AMSRD-ARL-WM-TD Aberdeen Proving Ground, MD 21005-5066		8. PERFORMING ORGANIZATION REPORT NUMBER ARL-TR-3646		
9. SPONSORING/MONITORING AGENCY NAME(S) AND ADDRESS(ES)		10. SPONSOR/MONITOR'S ACRONYM(S) 11. SPONSOR/MONITOR'S REPORT NUMBER(S)		
12. DISTRIBUTION/AVAILABILITY STATEMENT Approved for public release; distribution is unlimited.				
13. SUPPLEMENTARY NOTES				
14. ABSTRACT Stability of robotic path tracking can be violated because of different reasons. One of those is the time lag in the control system. Like in many other engineering problems, it is desirable to use the regimes of exploitation of robotic systems with near-critical values of control parameters. When crossing boundaries of stability domains (in the space of control parameters), the system can deviate from the desired regime either slightly or strongly. In the former case, the boundary of the stability domain is called safe, in the latter—unsafe. When dealing with robotic systems working in the near-critical regimes, it is important to design relevant algorithms and control systems having safe boundaries only. In this report, the concept of safe boundaries of the stability domain is discussed regarding the time-lag driven destabilization of control systems. The first part of this report deals with the simplest models described by a single, first-order Ordinary Differential Equation with a retarded argument. More complex and sophisticated models will be analyzed in the forthcoming parts of the report. We demonstrate that when using currently popular Pure Pursuit algorithm of robot path tracking, the stability domain has unsafe boundary. The problem of the boundary safety can be handled by switching to another algorithm of path tracking, which we coined as a “Hit-the-Road” algorithm.				
15. SUBJECT TERMS unmanned vehicles, path planning, time lag				
16. SECURITY CLASSIFICATION OF: UNCLASSIFIED		17. LIMITATION OF ABSTRACT UL	18. NUMBER OF PAGES 32	19a. NAME OF RESPONSIBLE PERSON Michael Grinfeld
a. REPORT UNCLASSIFIED	b. ABSTRACT UNCLASSIFIED			c. THIS PAGE UNCLASSIFIED

Contents

List of Figures	iv
1. Introduction	1
2. The Simplest Models of Path Tracking	2
2.1 The “Pure Pursuit” for Boating (PPB-Algorithms).....	3
2.2 The “Hit-the-Road” (HR) Algorithms.....	5
3. A Delay-Free Control	5
4. Delay-Triggered Instability of Deterministic Control	8
4.1 Linear Control Without Instantaneous Controllers	8
4.2 Numerical Analysis	10
4.3 Stabilization of Path Tracking by Adding an Instantaneous Controller.....	11
5. Nonlinear Effects in Delay-Triggered Unstable Control	12
5.1 The “Pure Pursuit for Boating” Controls With Delay.....	12
5.2 The PPB-1 Deterministic Control With Delay	13
5.3 The PPB-2 Deterministic Control With Delay	13
5.4 The PPB-3 Deterministic Control With Delay	14
5.5 How to Choose an Appropriate Look-Ahead Distance.....	15
6. The “Hit the Road” Deterministic Control With Delay	17
7. Conclusion	19
8. References	21
Appendix. Stability Analysis of Control Based on the Lyapunov Direct Method	23
Distribution List	25

List of Figures

Figure 1. The geometry of robotic vehicle path tracking.....	2
Figure 2. Three algorithms of a “pure pursuit for boating.”	4
Figure 3. Trajectories for three exponential deterministic delay-free controls.....	7
Figure 4. An UGV’s trajectory for a linear stochastic delay-free control.	8
Figure 5. A linear deterministic control with delay for three rates of approaching.....	11
Figure 6. The PPB-2 deterministic control with delay for three rates of approaching.....	14
Figure 7. The PPB-3 deterministic control with delay.	15
Figure 8. Towards choosing an appropriate look-ahead distance in the PPB-3 algorithm.....	16
Figure 9. Maximum total velocity as function of maximum allowable deviation in the PPB-3 algorithm.....	17
Figure 10. Three graphs of $F(z) = H \arctan(\Gamma z)$	18
Figure 11. HR deterministic control with delay for three rates of approaching.	19
Figure 12. Maximum deviation from targeted path in the Hit the Road control.	20

1. Introduction

Stable path tracking is one of the central problems in robotics. The topic of robotic path tracking includes many branches with hundreds of academic and engineering publications. Suggested numerical algorithms of path tracking have already become so complex and sophisticated that rigorous mathematical analysis of the underlying engineering ideas is hardly possible. There is, however, a necessity to have several mathematically manageable models which can be used as benchmarks for validating numerous suggested algorithms.

Like in many other engineering problems, it is desirable to use the regimes of exploitation of robotic systems with near-critical values of control parameters. When crossing boundaries of stability domains (in the space of control parameters), the system can deviate from the desired regime either slightly or strongly. In the former case, the boundary of the stability domain is called safe, in the latter it is called unsafe. When dealing with robotic systems working in the near-critical regimes, it is important to design relevant algorithms and control systems having safe boundaries only. For the simplest models of mechanical systems, the concept of the safety of stability boundaries was developed in the 1940s by Russian mathematician and engineer N. N. Bautin. (See Andronov et al. (1) and references therein.)

One of the sources of complexity of suggested models stems from the fact that the robotic vehicles are modeled as solid bodies of finite size (bicycles or cars) rather than material points. Obviously, the models of finite size are closer to real vehicles than their point-like counterparts. In many respects, point-like models cannot compete with the finite-size models. On the other hand, some important experimental and theoretical phenomena have minor relations to the finite-size features of the model and they show up in the point-like models as well. In these cases, the point-like models have a serious advantage by providing the possibility of deep theoretical analysis. In the first part of the report, we review certain problems of this sort. Clear understanding of the problems and possibilities for the point-like models can help us to shape a realistic picture for the potential achievements concerning the finite size models of robots and of their path tracking abilities.

The simplest models of systems with delay are based on Ordinary Differential Equations (ODEs). These models have been intensively studied during several decades. Relating mathematical methods and results are summarized in (2–11). Some of these methods and models have been used for developing algorithms of path tracking (12–18). The simplest and most popular of these algorithms, called Pure Pursuit (PP), has been intensively studied in paper (12) and in many publications triggered by it. More recently, the PP-based algorithms faced serious obstacles triggered by the time-lag in the control. We discuss this instability and suggest another algorithm – called “Hit-the-Road” (HR) – which will hopefully be helpful to overcome the instability.

2. The Simplest Models of Path Tracking

In what follows, Unmanned Ground Vehicles (UGVs) and their paths are modeled as material points and mathematical curves, respectively, in a plane. In the (x, z) plane, let us consider a point P that has an assignment of moving along the x -axis with the constant speed V (see figure 1). We assume that the coordinates are dimensionless and are measured in appropriate units. For instance, it is natural to measure z in terms of a typical width of the road.

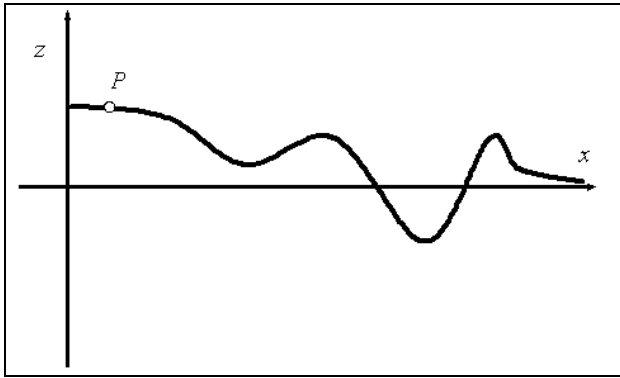


Figure 1. The geometry of robotic vehicle path tracking.

In fact, because of various uncontrolled disturbances, its path experiences some perturbations which should be kept as small as possible. Different algorithms of control have been suggested to keep the perturbations small enough. Let us consider the simplest control algorithm, which we will refer to as “normal return.” According to this algorithm, the vehicles maintain a constant horizontal velocity, $V = dx/dt$, along the x -axis, whereas its vertical velocity dz/dt is always directed towards the z -axis and depends on the distance z from this axis.

$$\frac{dz(t)}{dt} = a(z(t)). \quad (1)$$

The function $a(z)$ can be either linear (linear control) or nonlinear (nonlinear control). In fact, there is a natural time-delay τ in any control system. Therefore, instead of the ODE equation 1 we have to deal with the differential-delay equation (DDE)

$$\frac{dz(t)}{dt} = a(z(t - \tau)). \quad (2)$$

There is always a stochastic component in the vehicle motion that can be either big or small. This component can be modeled by adding a stochastic perturbation $\pi(t)$ to the RHS of equation 2.

$$\frac{dz(t)}{dt} = a(z(t - \tau)) + \pi(t). \quad (3)$$

Alternatively, certain stochastic behavior can be triggered by indeterminacy in the available information of the terrain or in the time-lag characteristics τ .

The simplest deterministic control functions of interest are the two-parameter power functions defined as

$$a(z) = -\frac{1}{T}|z|^m \operatorname{sign}(z), \quad (4)$$

with a positive constant T and non-negative m .

Because of the time-lag τ , the equations similar to equation 2 demand the initial data specified on the whole interval $(-\tau \leq t \leq 0)$ rather than at a single point:

$$z(t) = Z_0(t) \text{ at } -\tau \leq t \leq 0, \quad (5)$$

where $z_0(t)$ is a given function. At zero time-lag $\tau = 0$ the initial condition equation 5 reduces to the standard one: $z(0) = Z_0$.

Another nonlinear model of interest is called *ATAN*-model. We define it by the equation

$$a(z) = -H \arctan(\Gamma z), \quad (6)$$

where H and Γ are certain positive constants.

2.1 The “Pure Pursuit” for Boating (PPB-Algorithms)

The pure-pursuit algorithms for UGVs have been intensively studied in many publications (12–19). They rely on the so-called “bicycle” model of UGV. The algorithm is formulated in terms of an appropriate choice of the radius of curvature of the trajectory to be chosen. The key element of any pure-pursuit algorithm is the notion of the look-ahead distance L . In our one-dimensional point-like model we dwell on several analogies of the pure-pursuit algorithms. We call them “Pure Pursuit for Boating” (PPB). In order to justify this name, one has to imagine a power boat with a motor in the rear end and the front end raised high above the sea level. In this situation, the keel plays secondary role. The direction and speed of propulsion of the boat is determined by the power of the motor and by direction of its thrust. We consider three schemes of PPB; they are justified in figure 2.

The first PPB algorithm is shown schematically in the first column of figure 2. The motor enforces the constant total speed of V and the constant look-ahead distance L between the current point and the “rabbit” point on the targeted path: $z = 0$. Then, simple trigonometry leads to the following formula of the vertical velocity V_z :

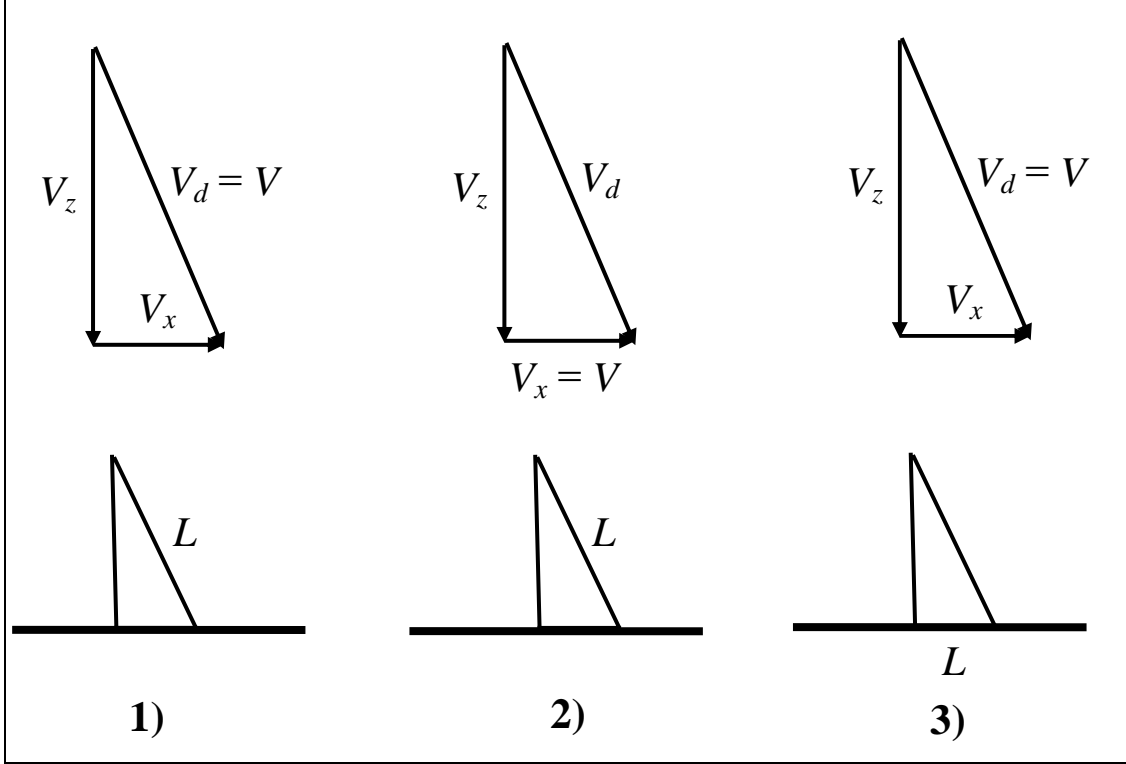


Figure 2. Three algorithms of a “pure pursuit for boating.”

$$V_z = a(z) = -\frac{V}{L} z. \quad (7)$$

The second PPB algorithm is shown schematically in the second column of figure 2. There is only one difference of PPB-2 from PPB-1: in PPB-2 the motor enforces the constant propulsion speed $V_x = V$. Then, simple trigonometry leads to the following formula of the vertical velocity V_z :

$$V_z = a(z) = -\frac{V}{L} \frac{z}{\sqrt{1 - \frac{z^2}{L^2}}}. \quad (8)$$

The third PPB algorithm is shown schematically in the third column of figure 2. In PPB-3, the look-ahead L is the distance between the “rabbit” and the projection of the current position (rather than the position itself) on the targeted x -axis. Then, simple trigonometry leads to the following formula of the vertical velocity V_z :

$$V_z = a(z) = -\frac{V}{L} \frac{z}{\sqrt{1 + \frac{z^2}{L^2}}}. \quad (9)$$

The same trigonometry leads to the following formula of the propulsion velocity V_x :

$$V_x = V_z \frac{L}{z} = \frac{V}{\sqrt{1 + \frac{z^2}{L^2}}}. \quad (10)$$

The PPB-2 and PPB-3 algorithms appear to be nonlinear in z . For sufficiently small values of z , they both reduce to the linear PPB-1 algorithm. For sufficiently large z , however, all three algorithms describe qualitatively different behaviors.

2.2 The “Hit-the-Road” (HR) Algorithms

The following suggested HR algorithms differ qualitatively from the PPB algorithms. It does not include anything like the look-ahead distance parameter. The main idea of HR algorithms is extremely simple: the propulsion velocity V_x has no relation whatsoever to the delay-driven destabilization of the path-tracking control. On the contrary, the transverse component of the velocity V_z is of key importance in what concerns the delay-driven destabilization. Thus, an appropriate algorithm of it should be chosen very carefully. In what follows, for this component we will choose one of the two-parameter sets of the ATAN functions. In other words, this sort of control is described by the ODE

$$\frac{dz(t)}{dt} = -H \arctan(\Gamma z(t)) \quad (11)$$

or by its delay-sensitive version

$$\frac{dz(t)}{dt} = -H \arctan(\Gamma z(t - \tau)). \quad (12)$$

There are two main sources of noise in such a system. One, $\tau_z(t)$, is in the indeterminacy of the z coordinate; the other, $\tau_\Delta(t)$, is in the indeterminacy of the delay τ . The corresponding ODE reads

$$\frac{dz(t)}{dt} = -H \arctan(\Gamma z(t - \tau - \pi_\Delta(t))) + \pi_z(t). \quad (13)$$

3. A Delay-Free Control

When dealing with the delay-free control, we arrive at the equation

$$\frac{dz(t)}{dt} = a(z(t)) + \pi(t). \quad (14)$$

Example 1: Nonstochastic control

In this case, we arrive at the initial-value problem

$$\frac{dz(t)}{dt} = a(z(t)), \quad z(0) = Z_0. \quad (15)$$

For the power-function models (equation 4), the last equation reads

$$\frac{dz(t)}{dt} = -\frac{1}{T} |z|^m \operatorname{sign}(z),$$

or else

$$\begin{cases} \frac{dz(t)}{dt} = -\frac{1}{T} z^m & \text{at } z > 0 \\ \frac{dz(t)}{dt} = -\frac{1}{T} (-z)^m & \text{at } z < 0 \end{cases}. \quad (16)$$

At $m = 1$, the Cauchy problem for equation 16 has the following solution:

$$z(t) = Z_0 e^{-\frac{t}{T}}. \quad (17)$$

The point returns back to its path (i.e., to the point $z = 0$) at $z \rightarrow \infty$.

At $m = \frac{1}{2}$, we get for $Z_0 > 0$

$$z(t) = \left(\sqrt{Z_0} - \frac{t}{T} \right)^{\frac{1}{2}}. \quad (18)$$

The point returns back to its path within finite time-interval at $t \rightarrow T \sqrt{Z_0}$.

At $m = 2$, we get

$$z = \frac{1}{Z_0^{-1} + \frac{t}{T}}. \quad (19)$$

The point returns back to its path at $t \rightarrow \infty$, but it does this slower than at $m = 1$.

More generally, at $m \neq 0$, the solution reads

$$z = Z_0 \left[1 + (m-1)Z_0^{m-1} \frac{t}{T} \right]^{\frac{1}{-m+1}}. \quad (20)$$

At $0 < m < 1$, the point returns back at the moment

$$t_{return} = T \frac{Z_0^{(1-m)}}{1-m}. \quad (21)$$

The graph in figure 3 shows numerical solutions of equation 16 for $T = 1$, $Z_0 = 3$, and $m = 1/2$ (series 1), $m = 1$ (series 2), and $m = 2$ (series 3).

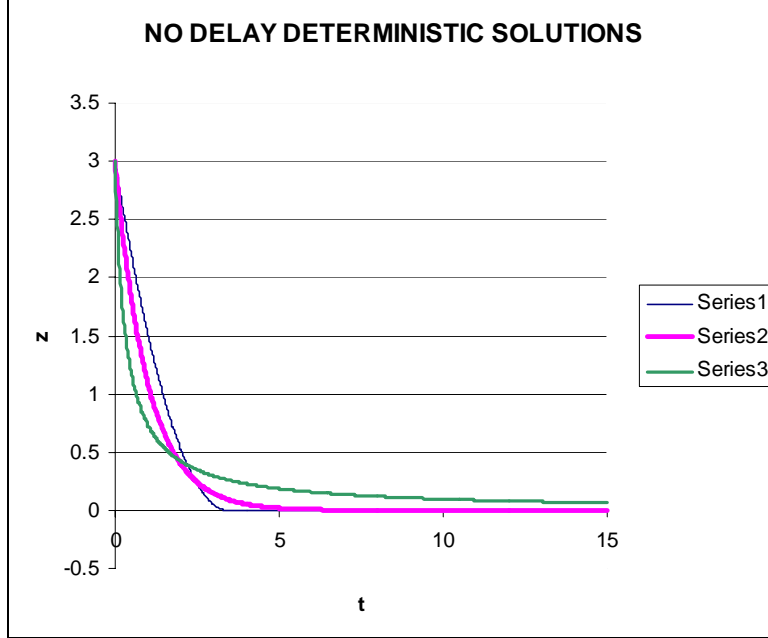


Figure 3. Trajectories for three exponential deterministic delay-free controls.

Example 2: Stochastic control at $m = 1$.

Stochastic control at $m = 1$ is described by the following system:

$$\frac{dz(t)}{dt} = -\frac{1}{T} z(t) + \pi(t), \quad z(0) = Z_0, \quad (22)$$

that can be integrated explicitly to read

$$z(t) = Z_0 e^{-\frac{t}{T}} + \int d\xi e^{\frac{\xi-t}{T}} \pi(\xi). \quad (23)$$

The graph in figure 4 shows the solution of equation 22 for the case $T = 1$, $Z_0 = 3$, and the stochastic perturbation $\pi(t)$ with the amplitude 0.1.

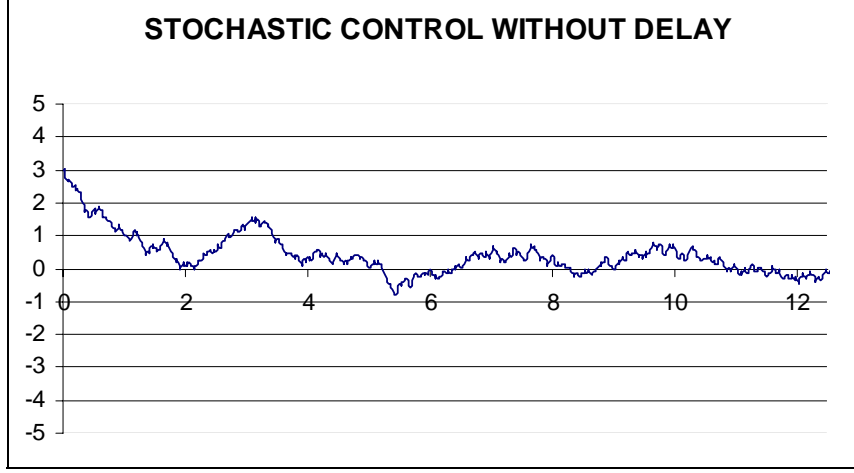


Figure 4. An UGV’s trajectory for a linear stochastic delay-free control.

4. Delay-Triggered Instability of Deterministic Control

4.1 Linear Control Without Instantaneous Controllers

A linear stochastic-free control is described by the system

$$\begin{aligned} \frac{dz(t)}{dt} &= -\frac{1}{T}z(t-\tau) \quad \text{at } t \geq 0 \\ z(t) &= Z_0 \quad \text{at } -\tau < t < 0. \end{aligned} \tag{24}$$

At $Z_0 = 0$, the system (equation 24) has the solution $z = 0$, usually called trivial solution. The stability concerns the behavior of the solutions at $Z_0 \neq 0$. If, for sufficiently small initial values of $|Z_0| \neq 0$, the corresponding solutions $z(t)$ are close to the trivial solution on the whole semi-infinite interval $-\tau < t < \infty$, then, the trivial solution is called stable. Otherwise, the trivial solution is called unstable.

In the absence of delay, the linear system $dz(t)/dt = -T^{-1}z(t)$ has the general solution $z = Ae^{-t/T}$ with the stable trivial solution $z = 0$. The presence of delay changes the situation dramatically. In systems with sufficiently large delay the trivial solution $z = 0$ appears to be unstable. Let us remind the classical facts of the theory of linear systems of ODE with delay. They can be found in any of the monographs (2–11).

Let us consider solutions of equation 24 of the form

$$z(t) = Ae^{pt}, \tag{25}$$

where A and p are certain constants. Combining equations 24 and 25, we arrive at the following transcendental equation for the exponent p :

$$Tp + e^{-\tau p} = 0. \quad (26)$$

Generally speaking, the roots p of the characteristic equation 26 are complex numbers depending on the parameters T and τ : $p = p(T, \tau)$. The function $p = p(T, \tau)$, generally speaking, has infinitely many branches. If one those roots has a positive real part, the solution equation 25 grows exponentially and the trivial solution $z = 0$ appears to be unstable.

Appearance of the roots with destabilizing real parts depends of the parameters T and τ . It is important to find in the parameter space (T, τ) the domains corresponding to the unstable behavior of the trivial solution, as well as boundaries of these domains. The boundary of the stability domain is defined by the equation

$$\operatorname{Re} p(T, \tau) = 0. \quad (27)$$

Equation 26 has infinitely many roots which cannot be calculated explicitly. In almost all practically sound engineering problems, the transcendental characteristic equations are even harder to solve. There is no chance whatsoever to solve them explicitly. Fortunately, it is much easier to make conclusions about the appearance of the unstable roots of the characteristic equations than to solve those equations explicitly. Some rather general mathematical results and engineering procedures in this direction have been established by Nyquist, Neiman, and Chebotarev (3, 5–7). For our transcendental equation 26, the boundary of the stability domain can be found by rather elementary calculations without any complex algebraic analysis. Using notation

$$\tau p = u, \tau / T = \gamma, \quad (28)$$

we can rewrite the original equation 26 as

$$u + \gamma e^{-u} = 0. \quad (29)$$

The classical equation 29 has been analyzed in hundreds of papers and several monographs including those of Pinney (2), Bellman and Cooke (3), Kolmanovskii and Myshkis (7), and others.

Looking for complex solutions of equation 29 in the form $u = x + iy$, we reduce this complex equation to the following pair of the real ones:

$$x + \gamma e^{-x} \cos y = 0, \quad y - \gamma e^{-x} \sin y = 0. \quad (30)$$

Let us find the boundary of the stability domain of the equation 29. According to the equation 27, the boundary can be determined from the condition

$$x = 0, \quad (31)$$

allowing to rewrite the system equation 30 as follows:

$$\gamma \cos y = 0, \quad y - \gamma \sin y = 0. \quad (32)$$

The system equation 32 allows one to find infinitely many (countable) number of critical values γ_n of the single parameter γ :

$$\gamma_n = \frac{\pi}{2} + 2\pi n, \quad (33)$$

where n is an arbitrary (positive or negative) digit. Corresponding critical imaginary parts are equal to

$$y_n = \pm \frac{\pi}{2} + 2\pi n. \quad (34)$$

Coming back to the original variables (T, τ) , we arrive at the following conditions of neutral stability:

$$\left(\frac{\tau}{T} \right)_n = \frac{\pi}{2} + 2\pi n. \quad (35)$$

By its physical meaning, only positive values of τ/T are of interest. The smallest of it is the following:

$$\left(\frac{\tau}{T} \right)_{crit} = \frac{\pi}{2}. \quad (36)$$

The criterion equation 36 implies the following strategy of stabilization of control: we have either to decrease the time-lag τ or, alternatively, to increase the constant T . Both approaches are in full agreement with engineering solutions in various applications, including robotic path tracking (12–17).

4.2 Numerical Analysis

The three graphs of the figure 5 show the trajectories of the controlling system obtained numerically for three different rates of approaching the desired position at $z = 0$. In principle, the results visualized in the figure could be obtained analytically for this simplest case. The possibility of the full theoretical analysis is rather an exception than the rule, especially when dealing with nonlinear control. Theoretical consideration, similar to that previously given, almost always permits analysis of the bifurcation and of the initial (linear) fraction of the unstable trajectory only. Further analysis of the unstable trajectory seems impossible without numerical methods.

LINEAR DETERMINISTIC CONTROL WITH DELAY

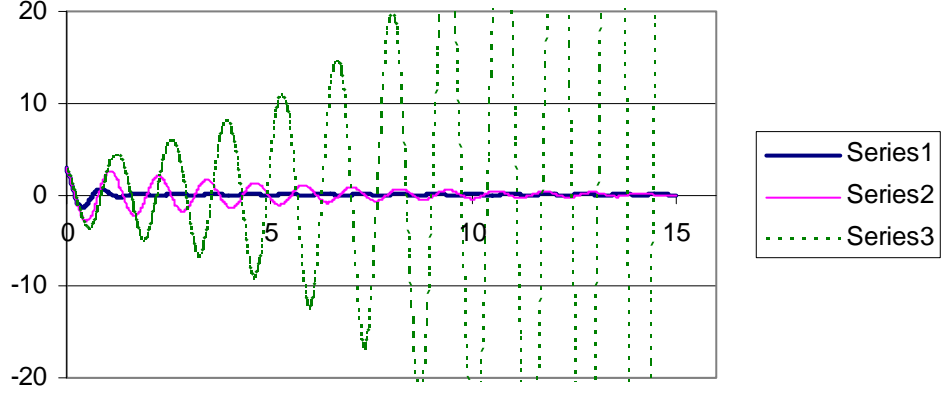


Figure 5. A linear deterministic control with delay for three rates of approaching.

The rate of approach for all three shown graphs is the same: $T^{-1} = 0.2$. Also, the initial deviation for all three graphs is the same: $z_0 = 3$. The only difference is in the choice of the delay τ . For the three series shown, it was chosen as $\tau_1 = 0.2$, $\tau_2 = 0.3$, and $\tau_3 = 0.5$, respectively. Per the stability criterion equation 36, for the first two regimes the solution $z = 0$ is stable, and for the last one it is unstable. The graphs clearly demonstrate these theoretical facts.

4.3 Stabilization of Path Tracking by Adding an Instantaneous Controller

Consider the following generalization of the ODE control described by the system equation 24:

$$\begin{aligned} \frac{dz(t)}{dt} &= Az(t) + B\bar{z}(t - \tau) \quad \text{at } t \geq 0 \\ z(t) &= Z_0 \quad \text{at } -\tau < t < 0. \end{aligned} \tag{37}$$

Constant A defines the instantaneous component of control, whereas B defines the delay component of control. At $A = 0$, we arrive at the situation analyzed earlier.

When looking for exponential solutions of the equation 37 instead of equation 24, then, instead of equation 25, we get

$$p - Be^{-\tau p} - A = 0. \tag{38}$$

Following the procedure of the previous section, instead of equation 30 we arrive at the following system of algebraic equations:

$$x - B\gamma e^{-\alpha x} \cos y - A = 0, \quad y - B\gamma e^{-\alpha x} \sin y = 0. \tag{39}$$

Let us find those A_n and B_n for which roots p_n appear to be purely imaginary. In this case, we get the following equations defining the boundary of neutral stability:

$$\cos y_n = -\frac{A_n}{B_n}, \quad y_n - B_n \sin y_n = 0, \quad (40)$$

implying

$$y_{n\pm} = \pm \arccos\left(-\frac{A}{B}\right) + 2\pi n. \quad (41)$$

The system equation 40 has no real solutions provided $|A/B| > 1$, and it does have real solutions otherwise. In other words, the delay-driven instability can be suppressed by adding to the control a sufficiently strong instantaneous component. More than that, given the amplitude B of the “delayed” ingredient of the controller, we can choose the appropriate amplitude A of the “instantaneous” component of controller which is able to suppress the instability with respect to any time delay.

5. Nonlinear Effects in Delay-Triggered Unstable Control

5.1 The “Pure Pursuit for Boating” Controls With Delay

Below we describe three different algorithms of pure pursuit which we call “Pure Pursuit for Boating” or PPB algorithms. From one hand, these algorithms resemble algorithms implemented earlier for UGV in several publications (12–16). On the other hand, they resemble control of a power boat when nose of the boat raised highly out of water and the motor dictates both: the direction of propulsion and the speed. Another analogy of the vehicle would be a circus “monocycle” with one wheel (as opposed to a standard bicycle with two wheels). The PPB-1 algorithm is linear, the PPB-2 and PPB-3 algorithms are nonlinear. In the linear approximation, however, all three of them are described by the same linear equation

$$\frac{dz(t)}{dt} = -\frac{V}{L} z(t - \tau), \quad (42)$$

where V is the vehicle speed and L is the so-called look-ahead distance. The stability criterion equation 36, then, dictates the constraint

$$\frac{V\tau}{L} \leq \frac{\pi}{2}. \quad (43)$$

or

$$V_{\max} = \frac{\pi L}{2\tau}. \quad (44)$$

Thus, the only ways to increase the maximum speed of stable propulsion are to decrease the time-lag τ or increase the look-ahead distance L . Both ways have their natural limitations. The time-lag is dictated by various engineering constraints. Choice of appropriate look-ahead distance is limited by the spatial scale of curvature of the preplanned path. These are conceptual limitations of various versions of the pure pursuit algorithms. To avoid these limitations, we suggest a conceptually different algorithm called “Hit the Road” or HR algorithm. This algorithm does not use the concept of lookahead distance, and, in principle, it permits a stable path tracking with arbitrary propulsion speed V .

5.2 The PPB-1 Deterministic Control With Delay

The PPB-1 control is described by the linear function equation 7: $V_z = a(z) = -\frac{V}{L}z$. Thus, the full theoretical analysis of the PPB-1 control with delay reduces to the analysis of the linear equation 24. Given the delay, this control appears to be stable for sufficiently large look-ahead distance L or for sufficiently small velocity V . Otherwise, the targeted solution $z(t) = 0$ appears to be unstable. In this case, the actual trajectory resembles the Series-3 of figure 5. However, not the entire curve-3 describes the unstable PPB-1 solution but only its initial fraction. This fraction covers the interval $0 < t < t^*$, where t^* is the moment of time at which the Series-3 crosses one of the horizontal lines $z = \pm L$. Obviously, at $t > t^*$ the PPT-1 algorithm fails.

5.3 The PPB-2 Deterministic Control With Delay

The PPB-2 control with delay is described by the function equation 8:

$$V_z = a(z) = -z \left(1 - \frac{z^2}{L^2}\right)^{-1/2} \frac{V}{L}. \text{ For small deviation from the targeted solution } z = 0, \text{ the}$$

nonlinear PPB-2 control reduces to the linear control PPB-1. Hence, the stability criteria for the two controls are the same. Contrary to the PPB-1 control, the analysis of unstable regimes for the PPB-2 requires numerical methods. Figure 6 shows three different trajectories for the PPB-2. All these trajectories start at the same initial position $z = z_0 = 0.01$, they have the same delay factor $\tau = 0.32$ and all of them have the same value of the parameter $A = V / L = 5$. For these parameters, the solution of the linear approximation is unstable.

The difference in the three graphs is implied by the choice of the parameter $h \equiv 1 / L^2$. For the red Series-1, the value of h is equal to 1. This solution disappears at $t \approx 1.22$ (see the red vertical line). For the Series-2, the value of h is equal 0.1. The solution disappears at a later moment of time (this moment is greater than 15, and it is not visible in the graph). At last,

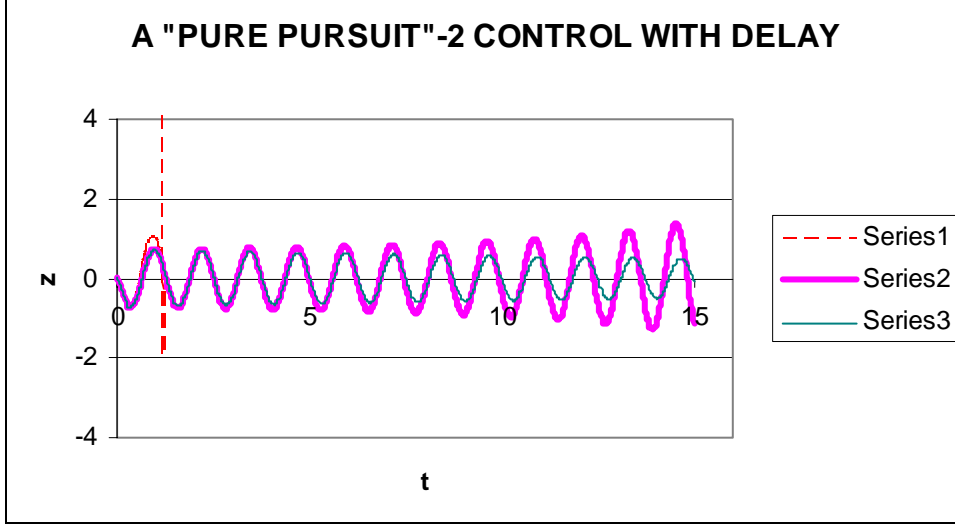


Figure 6. The PPB-2 deterministic control with delay for three rates of approaching.

for the Series-3, the value of h is equal to 0.01. Surprisingly enough, this solution seems to be stable. We do not have any justification for this nonlinearity-driven stabilization of the linearly unstable solution.

5.4 The PPB-3 Deterministic Control With Delay

The PPB-3 control with delay is described by the function equation 9:

$$V_z = a(z) = -z \left(1 + \frac{z^2}{L^2}\right)^{-1/2} \frac{V}{L}. \text{ Again, all these trajectories start at the same initial position}$$

$z = z_0 = 0.01$, they have the same delay factor $\tau = 0.4$, and all of them have the same value of the parameter $A = V / L = 5$. The three series shown correspond the values $h = 1, 0.1, 0.01$. All these solutions remain finite. The ratio $\rho \equiv V_z / V_x = z / L = z\sqrt{h}$ diminishes when h decreases. Still, it can be of a considerable magnitude. This means that a considerable loss of time and power can be implied by the PPB-3 control.

Let us consider regimes in which the UGV has the speed $V = \frac{(\pi + \varepsilon)L}{2\tau}$ slightly exceeding the

maximum stable speed $V_{\max} = \frac{\pi L}{2\tau}$ ($0 < \varepsilon \ll 1$). In this case, we get

$$V_z = a(z) = -\frac{\pi + \varepsilon}{2\tau} z \left(1 + \frac{z^2}{L^2}\right)^{-1/2}. \text{ In this situation, the delay-triggered instability shows up for}$$

any look-ahead distance L . Figure 7 demonstrates that the PPB-3 control implies appearance of oscillations of finite amplitude.

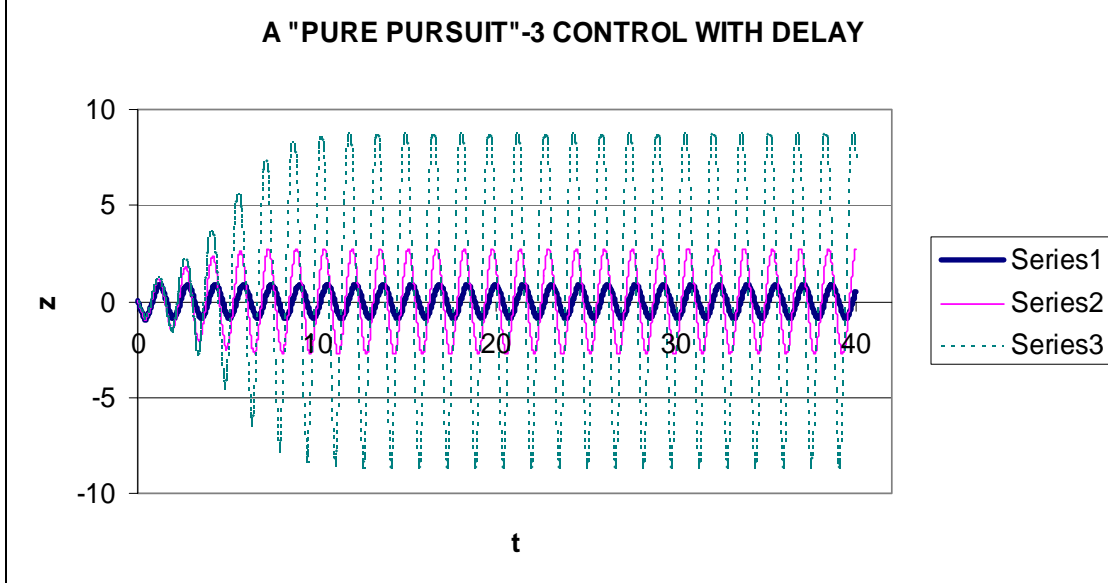


Figure 7. The PPB-3 deterministic control with delay.

5.5 How to Choose an Appropriate Look-Ahead Distance

The PPB-3 control with delay is closest of all three PPB to the traditional Pure Pursuit control for UGV. We can see that the PPB-3-control keeps the vehicle on a finite distance from the desired path after small accidental excess of the critical speed. We remind that destabilization of PPB-1 control leads to an unlimited growth of the deviation at $t \rightarrow \infty$. PPB-2control leads to an unlimited growth at t approaching certain (finite) moment of time. In fact, if the boundary of the stability region was crossed, both PPB-1 and PPB-2 controls fail after finite time interval: this happens because deviation from the pre-assigned path exceeds eventually the look-ahead distance. Thus, the stability boundary for the PPB-3 control is obviously safer than for PPB-1 and PPB-2 controls. On the other hand, the stability boundary for the PPB-3 control is still unsafe. For safety, small spontaneous deviation should imply arbitrarily small, but not finite, deviations of the robot in the interval $t \leq \infty$. This demand is certainly violated for the PPB-3 control.

To characterize this situation quantitatively, let us explore the maximal deviation of the UGV with PPB-3 control more carefully. The main question should be formulated as follows: given the look-ahead distance L , what is the maximum deviation of the UGV from the pre-assigned path when the velocity slightly exceeds its critical value V_{\max} ? The goal of this section is to explore the dependence of the amplitude upon the look-ahead distance. The maximum deviation of the vehicle from the desired path cannot be made arbitrarily small no matter how small the excess of the critical speed.

This problem can be addressed by means of direct numerical experiments based on numerical integration of the nonlinear equation

$$\frac{dz(t)}{dt} = -\frac{\pi + \varepsilon}{2\tau} z(t - \tau) \left(1 + \frac{z^2(t - \tau)}{L^2}\right)^{-1/2}. \quad (45)$$

How do we choose an appropriate or optimal look-ahead distance? First, we have to ensure that the UGV should be able to move as fast as possible. But there is the time-lag stability limitation. According to the formula (5b) – $V_{\max} = \pi L / 2\tau$, the bigger the desirable propulsion speed the bigger should be the look-ahead distance L . However, when the UGV incidentally (or deliberately) exceeds V_{\max} the delay-induced instability implied considerable deviation from the desired path. When destabilization occurs that the vehicle moves along an oscillatory path with growing amplitude and a specific frequency. We have a conjecture that the value of the frequency can be used as indicator of occurrence of the delay-triggered instability. This indicator can be used for subsequent adjustment of path-tracking parameters. It seems crucially important though to ensure that, until the adjustment takes place, the vehicle will not deviate too far from the pre-assigned path. The graphs on figure 3 suggest that the maximum instability-induced deviations grow with growth of the look-ahead distance L (or equivalently of V_{\max}). In other words, the bigger the look-ahead distance the more unsafe is the boundary of the stability domain in the parameter space. The implication of this discussion is very simple. The maximum look-ahead distance L should be chosen based on the maximum allowable deviation from the path. We determined the dependence of maximum deviation vs. look-ahead distance by making a series of numerical simulations. The results are shown in the figure 8.

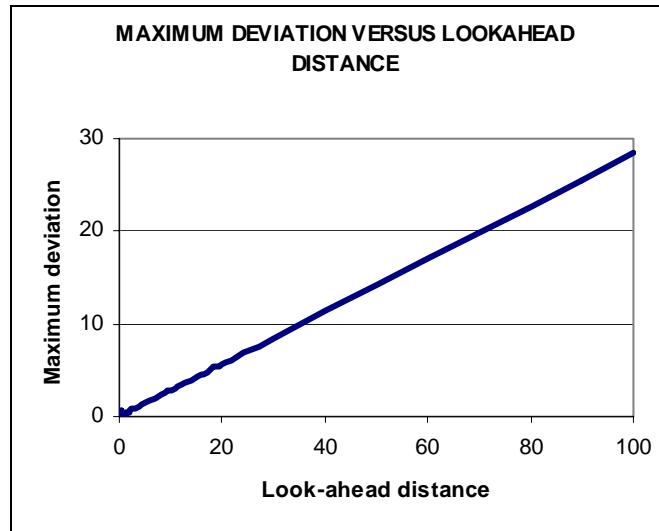


Figure 8. Towards choosing an appropriate look-ahead distance in the PPB-3 algorithm.

Figure 8 shows that for the PP-3 algorithm, the maximum deviation is approximately one third of the look-ahead distance.

Figure 9 gives the maximum velocity as function of maximum allowable deviation.

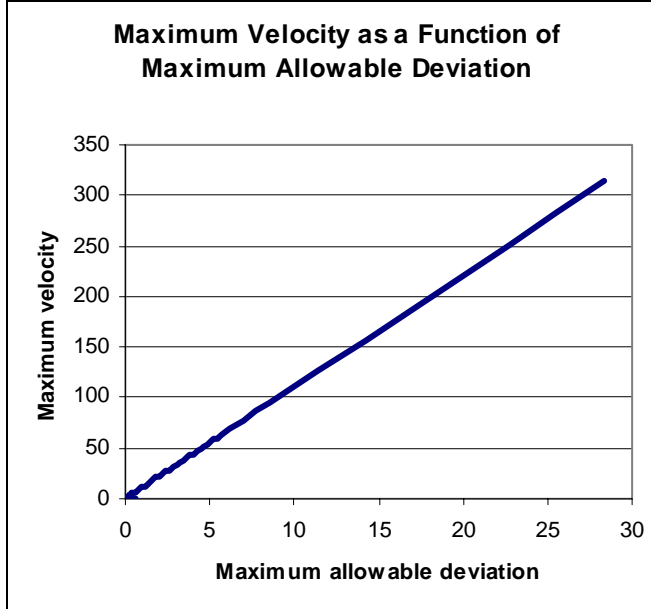


Figure 9. Maximum total velocity as function of maximum allowable deviation in the PPB-3 algorithm.

6. The “Hit the Road” Deterministic Control With Delay

As shown in the previous section, the demand of stability of the pure-pursuit algorithms imposes undesirable constraints on the admissible speed of stable propulsion of an UGV. In order to avoid those constraints, we suggest using conceptually different algorithms. The suggested HR algorithm does not use the notion of look-ahead distance at all. Also, this algorithm does not deal with the propulsion (tangential) component of the velocity—it can be arbitrarily large. Instead, it deals only with the normal component of the vehicle’s velocity, and the normal deviation $z(t)$ of the vehicle from the pre-assigned trajectory is the only quantity that matters. The HR deterministic control is a nonlinear ODE-based algorithm of control with delay. We suggest choosing a two-parameter function— $H \arctan(\Gamma z)$ —for the vehicle’s normal velocity. In other words, the suggested HR algorithm is described by the following first order ODE with delay:

$$\frac{\partial z(t)}{\partial t} = -H \arctan(\Gamma z(t - \tau)), \quad (46)$$

where H and Γ are certain positive constants.

Figure 10 shows the function $H \arctan(\Gamma z)$ for $H = 1$ and three different values of Γ : $\Gamma = 0.3$ (Series 1), $\Gamma = 1$ (Series 2), and $\Gamma = 10$ (Series 3).

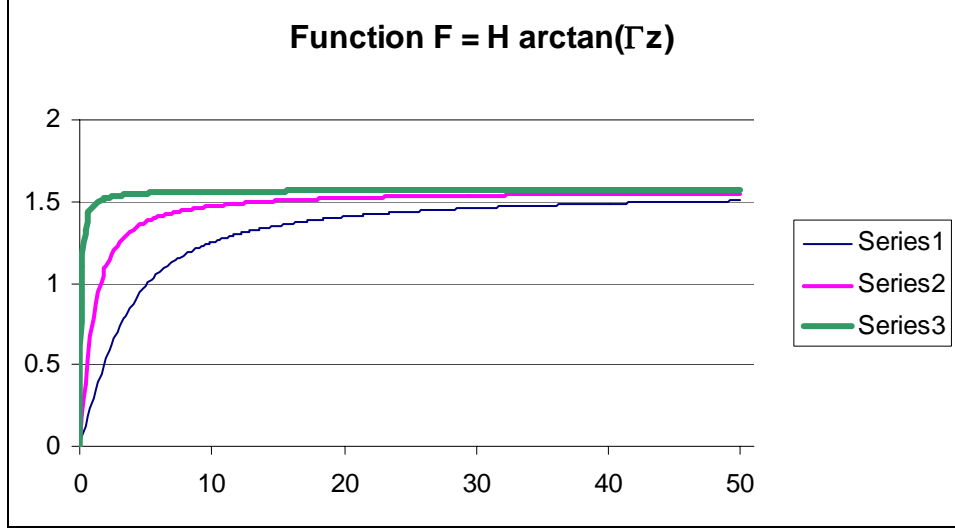


Figure 10. Three graphs of $F(z) = H \arctan(\Gamma z)$.

In linear approximation, equation 47 reads

$$\frac{\partial z(t)}{\partial t} = -H\Gamma z(t - \tau). \quad (47)$$

The stability condition for equation 47 can be obtained from equation 36. It reads

$$(\tau H \Gamma)_{crit} \leq \frac{\pi}{2}. \quad (48)$$

Figure 11 shows possible trajectories for the HR algorithm. All graphs are calculated for the same delay time $\tau = 0.36$, the same value of the parameter $H = 4$, and the same initial position $z = z_0 = 0.01$. The three series shown correspond to their different values of Γ : $\Gamma = 0.3$ (Series 1), $\Gamma = 1$ (Series 2), and $\Gamma = 10$ (Series 3).

The first regime is obviously stable, while the other two are unstable and lead to finite amplitude oscillations about the pre-planned path.

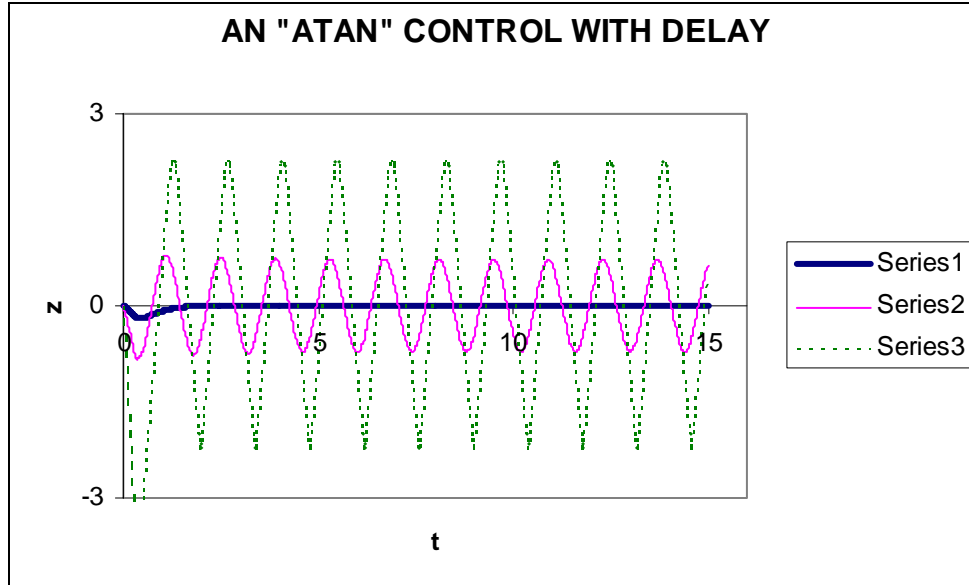


Figure 11. HR deterministic control with delay for three rates of approaching.

Similar to the PPB-3 algorithm, for planning an optimal choice of the parameters Γ and H we have to investigate maximum deviations of the unstable paths when intersecting the stable domain in the space of parameters (τ, Γ, H) . Regimes, close to the critical one, are described by the following equations:

$$\frac{\partial z(t)}{\partial t} = -\frac{\pi + \varepsilon}{2\tau\Gamma} \arctan(\Gamma z(t - \tau)), \quad (49)$$

or equivalently

$$\frac{\partial z(t)}{\partial t} = -H \arctan\left(\frac{\pi + \varepsilon}{2\tau H} z(t - \tau)\right), \quad (50)$$

where ε is a small parameter.

The graph in figure 12 shows the dependence of maximum normal deviation from the targeted path as function of the parameter H . The graph was built by means of numerical solving of equation 50 for $\Gamma = 5$, $A \equiv \frac{\pi + \varepsilon}{2\tau} = 3.3$.

7. Conclusion

Time lag in control leads to destabilization of path-tracking algorithms when parameters of the algorithms leave stability domains. Boundaries of stability domains in the parameter space for different algorithms can be either safe or unsafe. When crossing safe boundaries, the disturbed

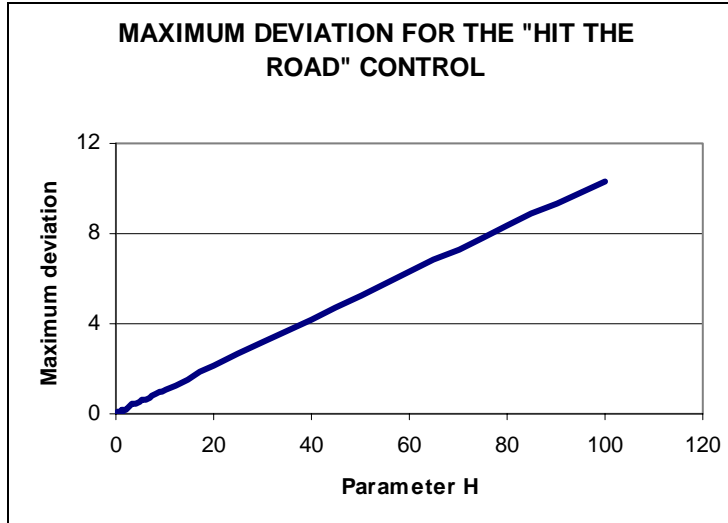


Figure 12. Maximum deviation from targeted path in the Hit the Road control.

path appears to be close to the pre-assigned one if the parameters stay close to the boundaries. When crossing unsafe boundaries, the path abruptly and strongly deviates far from the pre-assigned path. It is highly desirable to use algorithms of path tracking with the safe boundaries only. The previously mentioned analysis has demonstrated that traditional Pure-Pursuit algorithms, based on the concept of look-ahead distance, lead to the stability domains with unsafe boundaries. This fact imposes sensitive constraints on the maximum allowable propulsion velocity of UGV. To cope with this difficulty, we suggest using a novel HR algorithm. This algorithm does not use the concept of look-ahead distance and does not apply any stability constraints on the maximum propulsion velocity. This avenue of thought requires further studies and various efforts—mathematical, computational, and engineering.

8. References

1. Andronov, A. A.; Vitt, A. A.; Khaikin, S. E. *Theory of Oscillators*. Pergamon Press: Oxford, NY, 1966.
2. Pinney, E. *Ordinary Difference-Differential Equations*. University of California Press: 1958.
3. Bellman, R. E.; Cooke, K. L. *Differential-Difference Equations*. Academic Press: New York, NY, 1963.
4. Diekmann, O.; van Gils, S. A.; Verduyn-Lunel, S. M.; Walther, H. O. *Delay Equations, Functional, Complex and Nonlinear Analysis, Applied Math, Sciences Series, 110*; Springer-Verlag: New York, NY, 1995.
5. Gu, K.; Kharitonov, V. L.; Chen, J. *Stability and Robust Stability of Time-Delay Systems*. Birkhauser: Boston, MA, 2003.
6. Hale, J. K.; Verduyn Lunel, S. M. *Introduction to Functional Differential Equations*, Applied Math, Sciences, 99, Springer-Verlag: New York, NY, 1993.
7. Kolmanovskii, V. B.; Myshkis, A. D. *Applied Theory of Functional Differential Equations*. Kluwer, Dordrecht: The Netherlands, 1992.
8. Kuang, Y. *Delay Differential Equations With Applications in Population Dynamics*. Academic Press: Boston, MA, 1993.
9. Krasovskii, N. N. *Stability of Motion*. Stanford University Press: 1963.
10. MacDonald, N. *Biological Delay Systems: Linear Stability Theory*; Cambridge University Press: Cambridge, 1989.
11. Niculescu, S. I. *Delay Effects on Stability: A Robust Control Approach*, LNCIS; 269; Springer-Verlag: Heidelberg, 2001.
12. Amidi, O. *Integrated Mobile Robot Control*, M.S. Thesis, CMU, 1990.
13. Ollero, A.; Amidi, O. Predictive Path Tracking of Mobile Robots. Applications to the CMU Navlab. *Proceedings of the IEEE 5th International Conference on Advanced Robotics*, Pisa, 1991, pp 1081–1086.
14. Murphy, K. N. Analysis of Robotic Vehicle Steering and Controller Delay. *Proceedings of the 5th International Symposium on Robotics and Manufacturing*, Wailea, Maui, HI, 1994.

15. Murphy, K.; Legowik, S. GPS Aided Retro-Traverse for Unmanned Ground Vehicles. *SPIE 10th Annual AeroSense Symposium*, Orlando, FL, 1996.
16. Ollero, A.; Heredia, G. Stability Analysis of Mobile Robot Path Tracking. In *Proceedings of the 1995 IEEE/RSJ International Conference on Intelligent Robots and Systems*, Part 3 of 3. A Study of Polynomial Curvature Clothoid Paths for Motion Planning for Car-like Robots, Pittsburgh, PA, 1995, pp 461–466.
17. Pivtoraiko, M. *A Study of Polynomial Curvature Clothoid Paths for Motion Planning for Car-Like Robots*; CMU-RI-TR-04-68; Robotics Institute: Carnegie Mellon University, December 2004.
18. Yang, H.; Yang, S.; Mittal, G. Tracking Control of a Nonholonomic Mobile Robot by Integrating Feedback and Neural Dynamics Techniques. In *Proceedings of the 2003 IEEE International Conference on Intelligent Robots and Systems*, Las Vegas, NV, October 2003.
19. Wit, J.; Crane, C. D. Autonomous Ground Vehicle Path Tracking. *Journal of Robotic Systems* **2004**, 21 (8), 439–449.

Appendix. Stability Analysis of Control Based on the Lyapunov Direct Method

The analysis of stability of control systems with delay presented in this report and based on consideration of a characteristic function is applicable for linear control system only. There is another, alternative method of stability analysis called the Second, or Direct, method of Lyapunov. This method is a rather heuristic one and it does not have any systematic methodology. On the other hand, its applicability to various systems is not as sensitive to linearity as the system under study as the First method based on analysis of the characteristic equation. However, we demonstrate this method using the linear system and following the monograph of Krasovskii.¹

Let us consider the following time-dependent functional $L\{z(t)\}$ of the trajectory $z(t)$:

$$L\{z(t)\} = Iz^2(t) + D \int_{-\tau}^0 d\xi z^2(t + \tau), \quad (\text{A-1})$$

where $I > 0$ and $D > 0$ are certain positive constants. Treated as a function of t , the function $L\{z(t)\}$ is obviously positive.

$$L\{z(t)\} > 0 \quad \text{if } z(t) \neq 0. \quad (\text{A-2})$$

This is the first key relation required for validity of the Lyapunov direct method. The second one is the relationship

$$\frac{d}{dt} L\{z(t)\} < 0 \quad \text{if } z(t) \neq 0. \quad (\text{A-3})$$

With some additional (secondary) mathematical demands about $L\{z(t)\}$, the inequalities of equation A-2 and equation A-3 guarantee stability of the solution $z(t) = 0$.

Let us find the derivative $\frac{dL\{z(t)\}}{dt}$ along the trajectory of the system equation 37. Using the equation A-1, we get the following sequence of the relations:

¹Krasovskii, N. N. *Stability of Motion*. Stanford University Press: 1963.

$$\begin{aligned}
\frac{1}{2} \frac{dL\{z(t)\}}{dt} &= I_z(t) \frac{dz(t)}{dt} + D \int_{-\tau}^0 d\xi z(t+\xi) \frac{dz(t+\xi)}{dt} \\
&= I_z(t) [Az(t) + Bz(t-\tau)] + D \int_{-\tau}^0 d\xi z(t+\xi) \frac{dz(t+\xi)}{dt} \\
&= I_z(t) [Az(t) + Bz(t-\tau)] + \frac{D}{2} \int_{-\tau}^0 d\xi \frac{dz^2(t+\xi)}{dt} \\
&= I_z(t) [Az(t) + Bz(t-\tau)] + \frac{D}{2} z^2(t+\xi) \Big|_{-\tau}^0 \\
&= I_z(t) [Az(t) + Bz(t-\tau)] + \frac{D}{2} [z^2(t) - z^2(t-\tau)] \\
&= \left(AI + \frac{D}{2} \right) z^2(t) + BI_z(t) z(t-\tau) - \frac{D}{2} z^2(t-\tau). \tag{A-4}
\end{aligned}$$

The second stability inequality equation A-3 will be satisfied if one can find such positive constants as I and D such that

$$B^2 I^2 \leq -(2AD + D)D. \tag{A-5}$$

Such positive constants as I and D can be found if the “instantaneous control coefficient” A is negative and sufficiently large in the absolute value and the “lag control coefficient” B is sufficiently small in absolute value.

The direct method of Lyapunov delivers some sufficient conditions of stability which might be (and quite often are) very far from the necessary conditions of stability. The success depends quite often on luck in finding an appropriate Lyapunov function. From that standpoint, when dealing with linear systems, the analysis based on the study of the corresponding characteristic equation is much deeper. Unfortunately, the concept of characteristic equation fails when dealing with nonlinear systems, whereas the direct method of Lyapunov permits direct generalization for nonlinear cases.

NO. OF
COPIES ORGANIZATION

1 DEFENSE TECHNICAL
(PDF INFORMATION CTR
ONLY) DTIC OCA
8725 JOHN J KINGMAN RD
STE 0944
FORT BELVOIR VA 22060-6218

1 US ARMY RSRCH DEV &
ENGRG CMD
SYSTEMS OF SYSTEMS
INTEGRATION
AMSRD SS T
6000 6TH ST STE 100
FORT BELVOIR VA 22060-5608

1 INST FOR ADVNCED TCHNLGY
THE UNIV OF TEXAS
AT AUSTIN
3925 W BRAKER LN
AUSTIN TX 78759-5316

1 DIRECTOR
US ARMY RESEARCH LAB
IMNE ALC IMS
2800 POWDER MILL RD
ADELPHI MD 20783-1197

3 DIRECTOR
US ARMY RESEARCH LAB
AMSRD ARL CI OK TL
2800 POWDER MILL RD
ADELPHI MD 20783-1197

3 DIRECTOR
US ARMY RESEARCH LAB
AMSRD ARL CS IS T
2800 POWDER MILL RD
ADELPHI MD 20783-1197

ABERDEEN PROVING GROUND

1 DIR USARL
AMSRD ARL CI OK TP (BLDG 4600)

<u>NO. OF COPIES</u>	<u>ORGANIZATION</u>	<u>NO. OF COPIES</u>	<u>ORGANIZATION</u>
1	CARNEGIE MELLON UNIV ROBOTICS INSTITUTE O AMIDI 5000 FORBES AVE PITTSBURGH PA 15213	39	ABERDEEN PROVING GROUND DIR USARL AMSRD ARL WM J MCCUALEY J SMITH T WRIGHT AMSRD ARL WM BF M FIELDS S WILKERSON AMSRD ARL WM EG E SCHMIDT AMSRD ARL WM M B BURNS AMSRD ARL WM MD C FOUNTZOULAS G GAZONAS AMSRD ARL WM RP J BORNSTEIN C SHOEMAKER AMSRD ARL WM T S SCHOENFELD M ZOLTOSKI
1	CARNEGIE MELLON UNIV ROBOTICS INSTITUTE A STENTZ 5000 FORBES AVE PITTSBURGH PA 15213		
1	CARNEGIE MELLON UNIV ROBOTICS INSTITUTE M PIVTORAIKO 5000 FORBES AVE PITTSBURGH PA 15213		
1	ROBOTIC RESEARCH LLC K MURPHY 814 WEST DIAMOND AVE STE 301 GAITHERSBURG MD 20878		
1	ROBOTIC RESEARCH LLC A LACAZE 814 WEST DIAMOND AVE STE 301 GAITHERSBURG MD 20878		
1	ROGERS ENGRNG & ASSOC R ROGERS GAINESVILLE FL 32605		
1	UNIV OF FLORIDA CENTER FOR INTELLIGENT MACHINES AND ROBOTICS J WITT GAINESVILLE FL 32611		
1	UNIV OF FLORIDA CENTER FOR INTELLIGENT MACHINES AND ROBOTICS C CRANE III GAINESVILLE FL 32611		
1	UNIV OF FLORIDA CENTER FOR INTELLIGENT MACHINES AND ROBOTICS D ARMSTRONG GAINESVILLE FL 32611		